Supporting Information for

# In-Situ Coupling Strategy for Anchoring Monodisperse $Co_9S_8$ Nanoparticles on S and N Dual-Doped Graphene as a Bifunctional Electrocatalyst for Rechargeable Zn-Air Battery

Qi Shao[1], Jiaqi Liu[1], Qiong Wu[1], Qiang Li[1], Heng-guo Wang[1,*], Yanhui Li[1], Qian Duan[1,*]

School of Materials Science and Engineering, Changchun University of Science and Technology, Changchun 130022, People's Republic of China

*****Corresponding authors. E-mail: wanghengguo@cust.edu.cn (H.G. Wang), duanqian88@hotmail.com (Q. Duan)

Tel: +86-431-85583176

## S1 Experimental Method

### S1.1 Materials

All chemical reagents (including $CoCl_2 \cdot 4H_2O$, ethanol, KOH, methanol, polyvinyl alcohol) were purchased from reliable sources (Aladdin Industrial Co., Shanghai; Sinopharm Chem. reagent Co. Ltd, China; Sigma Andrich) and used as received. All the chemicals were analytical grade in purity. Graphene oxide (GO) was synthesized by a modified Hummers Method [S1]. De-ionized water was obtained from an ultra-pure purification system. The zinc foil (99.98% metal basis) was obtained from Alfa Aesar and the light emitting diode (LED) (5 mm size, ~3 V), LED bike lamp (45×20 mm, 4.2 V) and LED scroll displaying screen (93 mm×32 mm, 4.7 V) were obtained from the local supplier.

### S1.2 Synthesis of 5, 10, 15, 20-Tetrakis (4-sodiosulfophenyl)-21H, 23H-Porphyrin (TSPP)

5, 10, 15, 20-Tetraphenyl-21H, 23H-porphyrin (TPP) was synthesized following the Adlers Method [S2]. TPP (0.5 g, 0.8 mmol) was dissolved in $H_2SO_4$ (17 mL, 0.32 mol) under reflux and heating conditions (120 °C) for 2h. After cooling to room temperature, the reaction mixture was poured into 300 mL deionized water and regulated the pH to 7-8 by using NaOH. Thereafter, the as-obtained solution was concentrated and filtered to remove the $Na_2SO_4$. Subsequently, the resulted solution was added into methanol and filtrated for several times to remove the precipitated $Na_2SO_4$. Finally, the crude compound was further purified by recrystallization from methanol and acetone for three times to obtain the purified TSPP.

### S1.3 Synthesis of Cobalt (II) 5, 10, 15, 20-tetrakis (4-sodiosulfophenyl)-21H, 23H-porphyrin (TSPPCo)

TSPP (0.2 g, 0.2 mmol) and $CoCl_2 \cdot 4H_2O$ (0.2 g, 1 mmol) were dissolved in 150 mL deionized water and heated to reflux for 4 h. After that, the mixture solution was concentrated and dissolved in methanol. At last, the resulted product was dried under vacuum for 12 h to obtain the TSPPCo.

## S1.4 Characterization

The microstructures of the nanomaterials were observed by scanning electron microscopy (SEM Hitachi S-4800) and transmission electron microscope (TEM) recorded on a Tecnai G2 operating at 200 kV. The crystal phases were evaluated by X-ray diffraction (XRD) patterns recorded on a Rigaku-Dmax 2500 diffractometer with Cu Ka radiation. FTIR measurements performed on a Bruker IFS 66V/S spectrometer using KBr pellets. X-ray photoelectron spectroscopy (XPS) analysis conducted with ESCALAB MK II X-ray instrument was used to analyze the composition of the nanomaterials. Raman spectra were collected with a Renishaw 2000 model confocal microscopy Raman spectrometer.

## S1.5 Electrochemical Measurements

The recorded potentials versus SCE were converted to a RHE scale based on the Nernst equation ($E_{RHE}=E_{SCE}+0.241+0.059pH$). To prepare the working electrode, 5 mg of $Co_9S_8$/NSG-700 was ultrasonically dispersed in ethanol (1 mL) with Nafion solution (50 μL) to generate a uniform ink. 10 μL of the catalyst slurry was dropped onto the surface of the electrode and then dried at the room temperature for the measurements of ORR/OER.

According to the LSV curves of ORR at the different potentials, the electron transfer number (n) was calculated according to the Koutecky-Levich (K-L) equations:

$$\frac{1}{J} = \frac{1}{J_D} + \frac{1}{J_K} = \frac{1}{B\omega^{1/2}} + \frac{1}{nFkC_{O_2}}$$

$$\mathrm{B} = 0.62\mathrm{nFC_{O_2}}\left(\mathrm{D_{O_2}}\right)^{2/3}\mathrm{v}^{-1/6}$$

Where J is the measured current density using RDE, while $J_D$ and $J_K$ are the diffusion- and kinetic-limiting current density, respectively. n is the number of transferred-electron per oxygen molecule and F is the Faraday constant (96,485 C $mol^{-1}$). In addition, ω reflects the rotation rate and k is the electron transfer rate constant. Meanwhile, B represents the slope of the following equation. Moreover, $C_{O_2}$ is the bulk concentration ($1.1\times10^{-3}$ mol $cm^{-3}$ for 0.5 M $H_2SO_4$ aqueous solution and $1.2\times10^{-3}$ mol $cm^{-3}$ for 0.1 M KOH aqueous solution), while the $D_{O_2}$ is the diffusion coefficient ($1.4\times10^{-5}$ $cm^2$ $s^{-1}$ for 0.5 M $H_2SO_4$ solution and $1.9\times10^{-5}$ $cm^2$ $s^{-1}$ for 0.1 M KOH solution). Besides, v is the kinetic viscosity of solution (0.01 $cm^2$ $s^{-1}$ for both 0.5 M $H_2SO_4$ solution and 0.1 M KOH solution).

## S2 Supplemental Figures

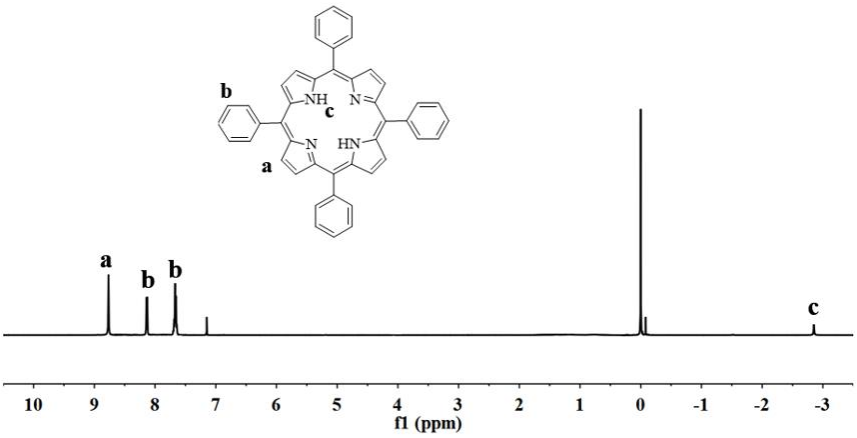


**Fig. S1** The $^{1}$H-NMR image of TPP

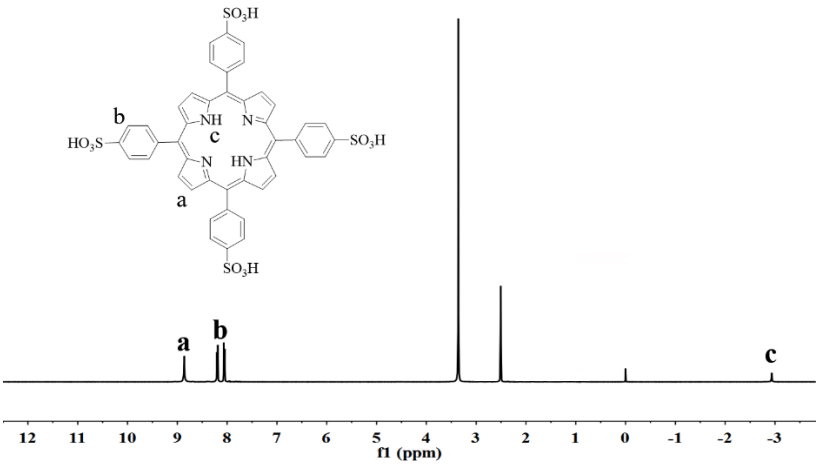


**Fig. S2** The $^{1}$H-NMR image of TSPP

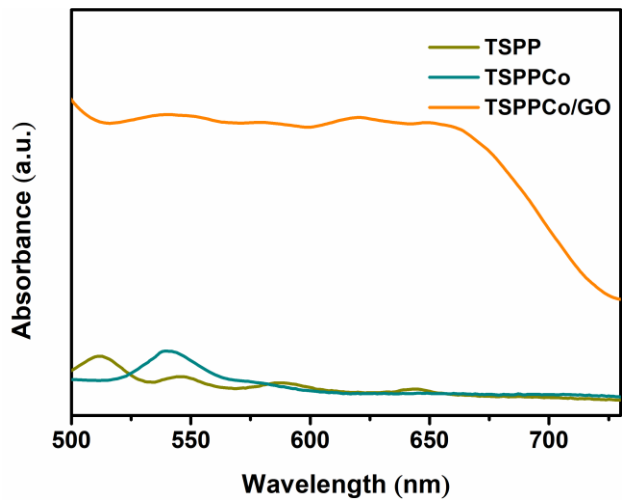


**Fig. S3** UV/Vis absorption spectra of TSPP, TSPPCo and TSPPCo/GO

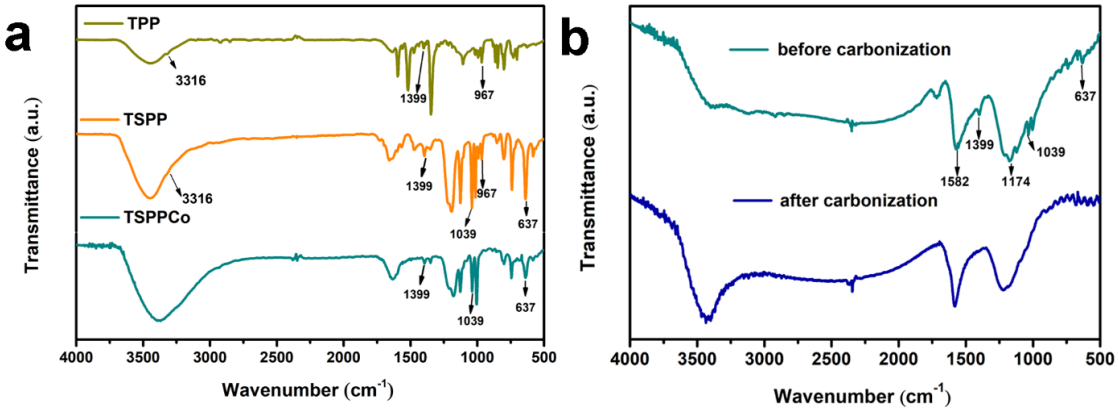


**Fig. S4 a** FTIR spectra of TPP, TSPP and TSPPCo. **b** FTIR spectra of $Co_9S_8$/NSG-700 before and after carbonization

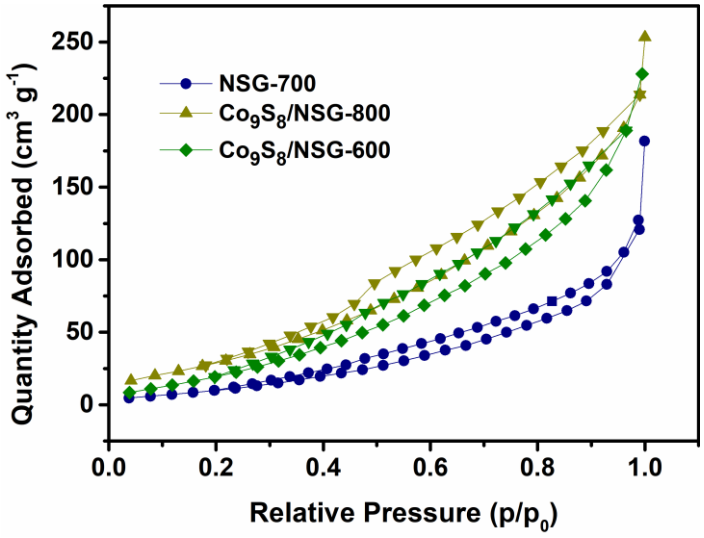


**Fig. S5** Nitrogen adsorption and desorption isotherms of NSG-700, $Co_9S_8$/NSG-600, and $Co_9S_8$/NSG-800

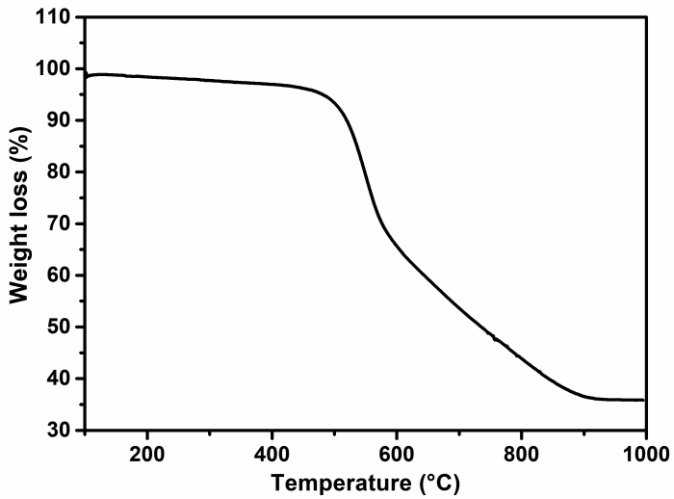


**Fig. S6** TG curve of $Co_9S_8$/NSG-700

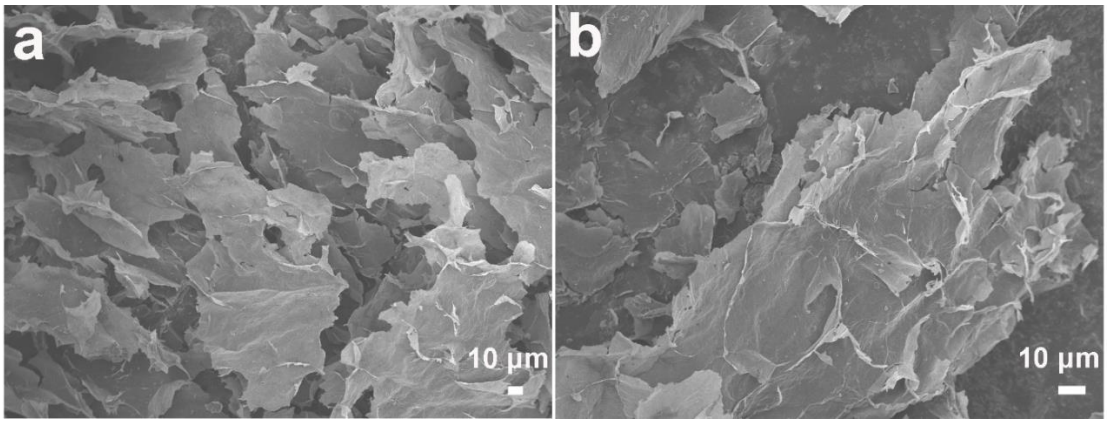


**Fig. S7** SEM images of **a** $Co_9S_8$/NSG-600 and **b** $Co_9S_8$/NSG-800

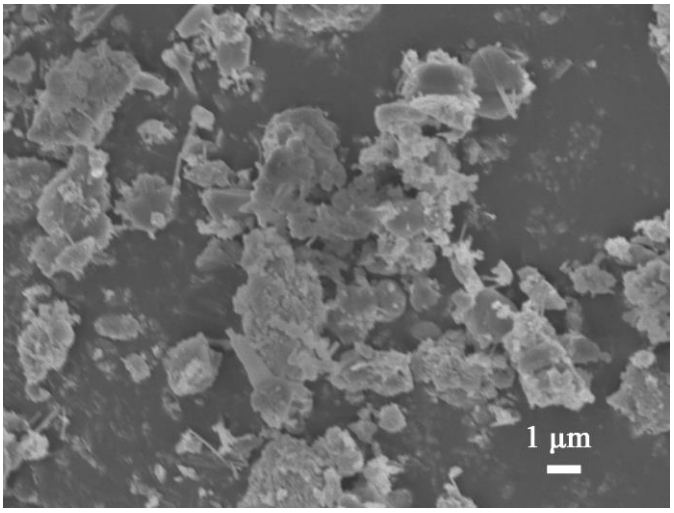


**Fig. S8** SEM image of $Co_9S_8$/C-700

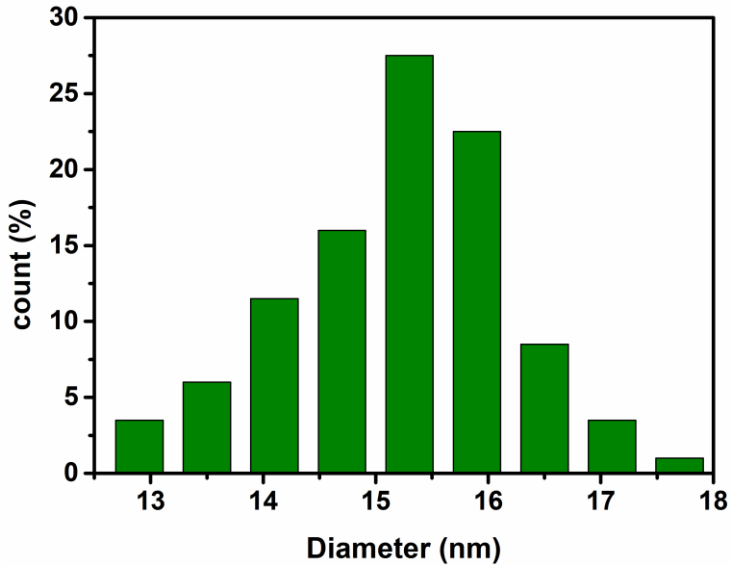


**Fig. S9** Particle size distribution of $Co_9S_8$/NSG-700

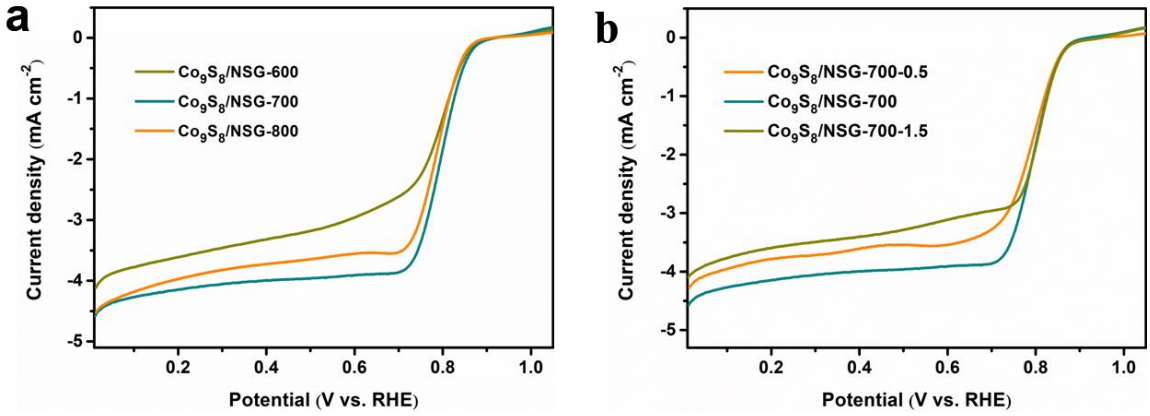


**Fig. S10** LSV curves of **a** $Co_9S_8$/NSG-600, $Co_9S_8$/NSG-700, $Co_9S_8$/NSG-800 and **b** $Co_9S_8$/NSG-700-0.5, $Co_9S_8$/NSG-700, $Co_9S_8$/NSG-700-1.5

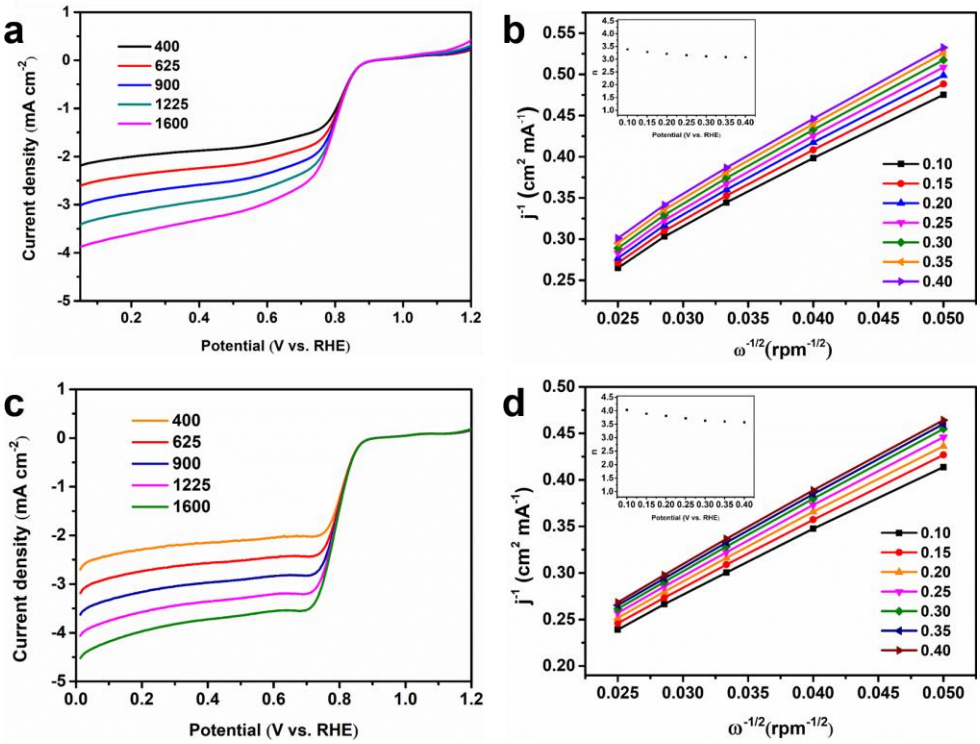


**Fig. S11 a** LSV curves of $Co_9S_8$/NSG-600 at different rotating rates. **b** K-L plots and the electron transfer number (insert) obtained from RDE results of $Co_9S_8$/NSG-600. **c** LSV curves of $Co_9S_8$/NSG-800 at different rotating rates. **d** K-L plots and the electron transfer number (insert) obtained from RDE results of $Co_9S_8$/NSG-800

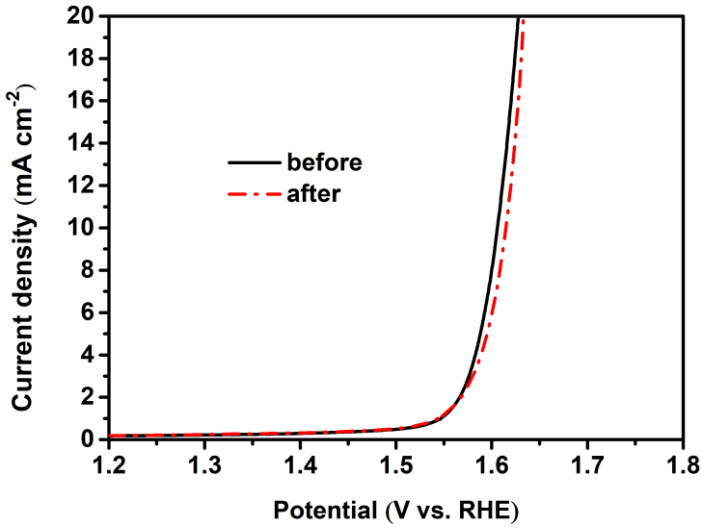


**Fig. S12** OER polarization curves of $Co_9S_8$/NSG-700 before and after a continuous 2000-cycle CV scan

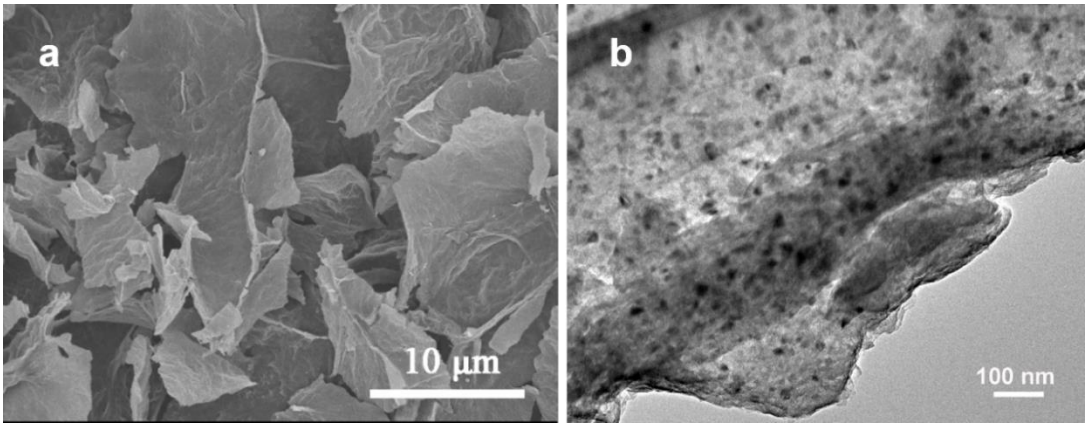


**Fig. S13 a** SEM image and **b** TEM image of $Co_9S_8$/NSG-700 after OER test

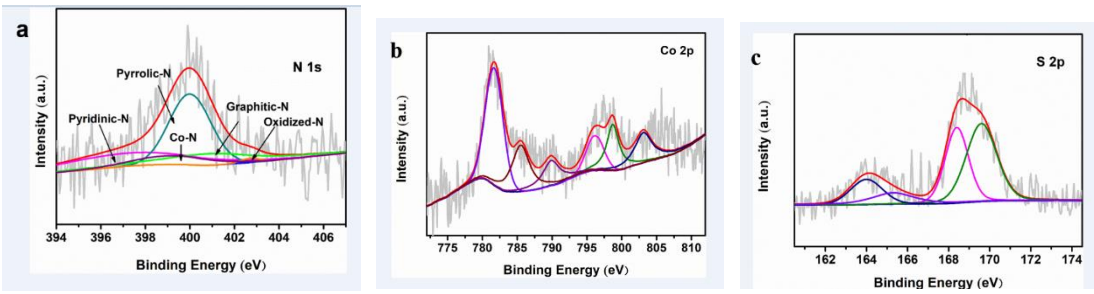


**Fig. S14** High resolution spectra: **a** N 1s, **b** Co 2p and **c** S 2p of $Co_9S_8$/NSG-700 after the OER catalytic process

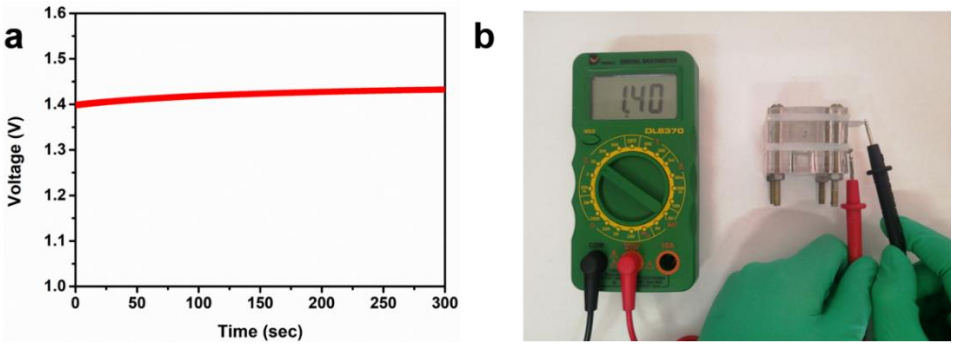


**Fig. S15 a** Open-circuit plots of assembled rechargeable Zn-air battery of Pt/C-$RuO_2$ catalysts. **b** Photograph of open-circuit potential

**Table S1** Elemental contents of C, O, N, S and Co in the $Co_9S_8$/NSG-700 before and after OER test determined by XPS analysis

| Catalyst | C (at%) | S (at%) | N (at%) | O (at%) | Co (at%) |
|---|---|---|---|---|---|
| $Co_9S_8$/NSG-700 before OER | 89.38 | 2.16 | 2.89 | 5.12 | 0.45 |
| $Co_9S_8$/NSG-700 after OER | 72.2 | 2.07 | 3.57 | 21.65 | 0.51 |

**Table S2** A survey of the catalytic performance of various bifuctional electrocatalysts

| Catalysts | Loading (mg $cm^{-2}$) | ORR | | OER | ΔE ($E_{j=10}$-$E_{1/2}$) (V) | References |
|---|---|---|---|---|---|---|
| | | $E_{onset}$ (V) | $E_{1/2}$ (V) | $E_{j=10}$ (V) | | |
| $Co_9S_8$/NSG | 0.25 | 0.92 | 0.79 | 1.61 | 0.82 | **This work** |
| $Co_9S_8$/NSPG | 0.283 | -- | 0.8 | 1.51 | 0.82 | **ACS Sustainable Chem. Eng.** 2017, 5, 9848-9857 |
| $Co_9S_8$@NSCM | 0.15 | 0.97 | 0.81 | 1.60 | 0.79 | **Nanoscale** 2018, 10, 2649-2657 |
| Co-N-pCNs | 0.25 | 0.96 | 0.80 | 1.63 | 0.83 | **ChemCatChem.** 2017, 9, 1601-1609 |
| N-GCNT/FeCo | 0.2 | 1.03 | 0.92 | 1.73 | 0.81 | **Adv. Energy Mater.** 2017, 7, 1602420 |
| $Co_3O_4$/NPGC | 0.2 | 0.97 | 0.84 | 1.68 | 0.84 | **Angew. Chem. Int. Ed.** 2016, 55, 4977-4982 |
| NiCo/PFC | 0.13 | 0.92 | 0.79 | 1.63 | 0.84 | **Nano Lett.** 2016, 16, 6516-6522 |
| $CoS_x$@PCN/rGO | 0.408 | -- | 0.78 | 1.57 | 0.79 | **Adv. Energy Mater.** 2018, 8, 1701642 |
| $CuCo_2S_4$ NSs | 0.2 | 0.90 | 0.70 | 1.52 | 0.82 | **Nanoscale** 2018, 10, 6581-6588 |

Notes: ORR and OER Data reported in these works are normalized into reversible hydrogen potential (RHE).

**Table S3** A survey of the performance of Zn-air batteries with various electrocatalysts

| Catalysts | Loading (mg $cm^{-2}$) | Peak Power (mW $cm^{-2}$) | Open circuit potential (V) | References |
|---|---|---|---|---|
| $Co_9S_8$/NSG | 1.0 | 72.4 | 1.42 | **This work** |
| N-GRW | 0.5 | 65 | 1.46 | **Sci. Adv.** 2016, 2, e1501122 |
| N-CN9 | 1.0 | 41 | 1.13 | **Electrochim. Acta.** 2017, 247, 1044-1051 |
| NPMC | 0.5 | 55 | 1.48 | **Nat. Nanotech.** 2015, 10, 444-452 |
| S, N-Fe/N/C-CNT | 1.25 | 102.7 | 1.35 | **Angew. Chem. Int. Ed.** 2017, 56, 610-614 |
| N8-VA-CNTs/GF | 1.3 | 67 | 1.45 | **J. Mater. Chem. A** 2017, 5, 2488-2495 |
| c-$CoMn_2$/C | 2.0 | 79 | -- | **Nat. Commun.** 2015, 6, 7345 |
| NiFeO@$MnO_x$ | 0.25 | 81 | 1.32 | **ACS Appl. Mater. Interfaces** 2017, 9, 8121-8133 |
| Fe@C-NG/NCNT | 1.0 | 101.3 | 1.37 | **J. Mater. Chem. A** 2018, 6, 516-526 |

## S3 References


[S1] W.S. Hummers, R.E. Offeman. Preparation of graphitic oxide. J. Am. Chem. Soc. **80**(6), 1339 (1958). https://doi.org/10.1021/ja01539a017

[S2] A.D. Adler, F.R. Longo, J.D. Finarelli, J. Goldmacher, J. Assour, L. Korsakoff. A simplified synthesis for meso-tetraphenylporphine. J. Org. Chem. **32**(2), 476 (1967). https://doi.org/10.1021/jo01288a053